

SHORT-PERIOD SEISMIC RADIATION AND ESTIMATION OF STRONG MOTION FROM LARGE EARTHQUAKE

A.A.GUSEV^I and S.A.FEDOTOV^I

SUMMARY

Based on the assumption of the incoherence of large earthquake source radiation in short-period range, a simple theoretical model of radiation field is proposed. Using empirical data on average correlation of source parameters and source spectrum with seismic moment, this model was successfully tested. It allows us to predict peak acceleration, duration and intensity in the near field of large earthquake. Strong motion simulation technique is described based on this model.

INTRODUCTION

Seismic radiation from a source of large earthquake in the "engineering seismology" frequency range is predicted only poorly by deterministic source models. Adequate description is important as a theoretical basis for strong motion prediction. The existing empirical correlations of intensity and peak acceleration with magnitude and epicentral distance provide firm ground for testing such a description. After successful testing it can be used rather reliably for strong motion simulation.

SOURCE MODEL

On the basis of works of Haskell (1964), Aki (1967; 1972), Shebalin (1971) and Blandford (1975), we (Gusev, 1979) treat a large earthquake source incoherently radiating in a frequency range of 0.5-20 Hz as a population of "smooth" sub-sources having ω^{-5} spectra. Subsources in our model represent details of rupture propagation and fault wall sliding, including crack bifurcation and en-echelon propagation, fault wall interlocking and relative sliding of wavy surfaces. A double dipole or a simple compensated dipole (for the last case) can be taken as force equivalents for these subsources. The source spectrum in our model is determined from subsurface size distribution. The simplest hypothesis is that the length L distribution of subsources is the power law: $N(L) \sim L^{-\gamma}$ (Shebalin, 1971; see Anderws (1979) for a different model based on the similarity hypothesis). Yet real spectra demonstrate the existence of two characteristic lengths: $L_1 \sim 10$ km and $L_2 \sim 0.2 \pm 1$ km. Within the interval $L_2 < L < L_1$ the number of subsources, normalized with the power law distribution, is greater than outside this interval. This can be deduced from, for instance, two-humped P-wave velocity spectra of $M \sim 8$ earthquakes (Zapolskii et al., 1973) for L_1 and from Z-shaped form of spectrum scaling laws of Chouet et al. (1978) for L_2 . Thus, the simple similarity hypothesis for scaling spectra

^IInstitute of Volcanology, USSR Academy of Sciences, Petropavlovsk-Kamchatskii, 683006 USSR

fails. Making now no attempt to estimate the real subsurface density and derive a spectral shape from it, further we shall use empirical spectra only which underwent smoothing and averaging. These subsources will be considered as statistically independent, thus giving us an opportunity to consider radiation intensity. The earlier attempts to describe source radiation in this way were made by Rautian (1976) and Kopnichev and Shpilker (1978).

RADIANT FLUX STABILITY

As a first approximation we can suppose that short-period radiant flux W_{sp} from the unit source area is a certain constant, not depending upon the position of radiating point, time or magnitude. To test this assumption, correlations of magnitudes M_L , M_{LH} , M_S , source length L , mean slip B , characteristic time T and total radiated energy E with seismic moment value M_0 were constructed beforehand (Fig. 1) using data from various publications (full reference list will be given in the extended version of the report). Approximate relations $L \sim B \sim T \sim M_0^{1/5}$ for $\lg M_0 = 23 \div 29$ can be derived from the plotted curves. Then the average source radiation spectra in terms of moment spectrum of equivalent point source $M(f)$ were constructed (Fig. 2) based mainly on the results of Trifunac (1976) and $\beta(f)$ values of Zapol'skii et al. (1974). Now, using curves from Figs. 1 and 2, the radiant flux energy spectra $W(f) = \beta^3 E / \partial S \partial \log f$ were computed.

Using the approximate relation for the rectangle source,

$$W(f) = (2\pi \ln 10 v w \Delta \epsilon / 5 V_s^2) \cdot (f^3 M_0^2(f) / M_0) \quad (1)$$

where V_s is the Swave velocity, f is the frequency, $M_0 = M_0(0)$, v , w , $\Delta \epsilon$ are the dimensionless constants: U is the Mach number for the rupture velocity, w is the width to length ratio, $\Delta \epsilon$ is the strain drop. The accepted values are $V_s = 3.5$ km/s, $v = 0.6$, $w = 0.5$, $\Delta \epsilon = 1 \cdot 10^{-4}$. The right multiplier in Eq. 1 is plotted in Fig. 3. Integrating Eq. 1 from $f = 0.3$ Hz to infinity, we obtain $W_{sp} \approx 5 \cdot 10^7$ erg/cm²s for $\lg M_0 = 25 \div 28$ ($M_{LH} = 5 \div 8$). Real variations of W_{sp} are large, being half an order of magnitude or even greater. A significant part of these variations can be related to the source mechanism type (Gusev, 1979; Aptikaev and Kopnichev, 1979), namely reverse dip-slip sources radiate more intense than strike-slip ones.

RADIATION FIELD MODEL AND INTENSITY CURVES

Now we shall compare implications of our model with empirical data. Radiation field amplitude x of incoherently isotropically radiating disk of radius R for the point on its axis at distance r can be described by approximate formula

$$x^2 \sim \ln \left(\frac{R^2 + r^2}{R_c^2 + r^2} \right) \quad (2)$$

where $2R_c$ is the correlation length of the source. We used even a simpler approximation

$$x^2 \sim (1 + (r^2/R^2))^{-1/2} \quad (3)$$

for all directions. Now we can derive the theoretical relation between intensity I , magnitude M and hypocentral distance r . We shall accept

$$I = a \log A + b \log \tau + C \quad (4)$$

where $a = 3.3$, A is the peak acceleration. Strong shaking duration τ is supposed to be equal to source characteristic time T (Dobry et al., 1978). Their data on $\tau(M)$ practically coincide with T curve in Fig.1. Value $b = 0.9$ is a minimal estimate obtained from data of Aptikaev (1976). Let us accept then that $f = 2.5\text{Hz}$, $Q_s = 300$, $W_{sp} = \text{const}$, $R = 0.4L$, $\lg R = 1/3(\lg M_0 - 22.43)$ (Fig.1), $\lg T = 1/3 \lg M_0 + \text{const}$. Then

$$I = 3.3 \log [1 + (3.0 \cdot 10^7 r / M_0^{1/2})^2]^{-1/2} \cdot \exp(-0.009r) + 0.50 \log M_0 + C \quad (5)$$

(r in km, M_0 in dyne·cm). Fig.4, where relation $M_{LH}(M_0)$ was taken from Fig.1, demonstrates how predictions of our model match with Shebalin's standard linear relations $I(M,r) = 1.5M_{LH} - 3.5 \lg r + 3.0$ and $I_0 = I(M,0) = 0.4M_{LH} + 7.0$ (Seismicheskoye..., 1977). The best fit is obtained for $C = 1.83$. Deviations at $R = 100$ km can decrease, taking into account the wide-band frequency content of radiation, and are not very significant, and in other parts of the graph a mismatch is minimal.

Empirical relations $A(r, M)$ from Kramynin and Shteinberg (1976) or analogous data of Page et al. (1975) can be approximated equally good by Eq.3 with $R = R(M)$ when absorption is taken into account. We ought to note here the previous results of Hanks (1976) and Kramynin and Shteinberg (1976) who marked saturation of $A(r)$ relation when $r \rightarrow 0$ and of Dieterich (Page et al., 1975) who proposed to scale the $A(r)$ curves according to source dimension.

STRONG MOTION SIMULATION

The above results were used as a base for strong motion simulation system for a rock site. The flow chart of S-wave horizontal accelerogram simulation is illustrated in Fig. 5. The input data include 1. Seismic moment M_0 and distance r . 2. $M_0(f)$ and $T(M_0)$ according to Figs.1 and 2 or specially constructed. 3. Standard envelope function for dimensionless time t . Function $ENV(t) = t \exp(-t)$ was accepted. 4. Correction to $\log I$ in order to take into account non-standard $\Delta\sigma$ value. 5. Coefficient for mechanism and regional anomalies. 6. Amplitude curves $A_s(r)$ obtained from short-period observations in the region. 7. $Q_s(f)$. 8. Site spectral correction, including effects of acoustic stiffness difference between the site and source regions. The way of computation becomes clear from Fig.5. The finiteness correction is computed according to Eq.3. Two test examples of program output are plotted in Fig.6. The simulation system will be completed in 1980.

The above computation technique is rather simplified. The main effects not taken into account are 1. Surface and scattered waves. 2. $W(f)$ variations with position on the fault (depth firstly), time, M , and $\Delta\sigma$. 3. Increase of duration with distance. 4. Effects of partial coherence of radiation. 5. Non-radiating ("static") oscillations in a very near field. Nevertheless, we suppose that the described technique can be considered to be the useful first approximation for prediction of engineering effects of large earthquake, as it is based on the seismic moment scale and clear physical assumptions. Our approach to simulation of realistic strong motion can be compared with another technique developed by Kopnischev et al. (1979).

CONCLUSIONS

1. Inapplicability of source similarity hypothesis for extrapolation of short-period large earthquake spectra is revealed.
2. Average empirical relations of earthquake source parameters and source spectrum with seismic moment value are constructed.
3. Relative stability of short-period radiation flux from the unit source area is shown.
4. An approximate formula is suggested to describe amplitudes in the near field of radiation of finite source.
5. Theoretical relation between seismic intensity, magnitude and distance is derived which agrees with empirical dependence.
6. A simplified technique for realistic strong motion simulation is proposed.

REFERENCES

- Aki, K., 1967. Scaling law of seismic spectrum. *J. Geophys. Res.*, v.72, p.1217-1231.
- Aki, K., 1972. Scaling law of earthquake source time-function. *Geophys. J.*, v.31, p.3-25.
- Andrews, D.J., 1979. A stochastic fault model. (Preprint).
- Aptikaev, F.F., 1976. Consideration of duration of vibration in instrumental estimation of seismic intensity. In: *Seismicheskaya Shkala i Metody Izmereniya Seismicheskoi Intensivnosti*. Moscow, Nauka, p. 234-239 (in Russian).
- Aptikaev, F.F. and Kopnischev, Yu.F., 1979. Consideration of earthquake source mechanism in prediction of strong motion parameters. *Doklady AN SSSR*, v.247, p.822-825 (in Russian).
- Blandford, R.R., 1975. A source theory for complex earthquakes. *Bull. Seismol. Soc. Amer.*, v.65, p.1385-1405.
- Chouet, B., Aki, K. and Tsujiura, M., 1978. Regional variation of the scaling law of earthquake source spectra. *Bull. Seismol. Soc. Amer.*, v.68, p. 49-79.

- Dobry, R., Idriss, I.M. and Ng, E., 1978. Duration characteristics of horizontal components of strong-motion earthquake records. Bull. Seismol. Soc. Amer., v.68, p.1487-1520.
- Gusev, A.A., 1979. A simple descriptive model of earthquake source short-period radiation. Doklady ANSSSR, v. 244, p.544-548 (in Russian).
- Haskell, N.A., 1964. Total energy and energy spectral density of elastic wave radiation from propagating faults. Bull. Seismol. Soc. Amer., v. 54, p. 1811-1841.
- Hanks, T.C. and Johnson, D.A., 1976. Geophysical assessment of peak accelerations. Bull. Seismol. Soc. Amer., v. 66, p.959-968.
- Kopnichev, Yu.F. and Shpilker, G.L., 1978. Parameters of high frequency source radiation and model of strong motion. Doklady AN SSSR, v.239, p.193-196 (in Russian).
- Kopnichev, Yu.F., Nersesov, I.L. and Shpilker, G.L., 1979. Simulation of the vertical component of accelerogram of the Gazli earthquake, May 17, 1976. Doklady AN SSSR, v. 246, p.40-43 (in Russian).
- Kramynin, P.I. and Shteinberg, V.V., 1976. Parameters of vibrations of dense soil in strong earthquakes. In: Voprosy Inzhenernoi Seismologii, No. 18, Moscow, Nauka, p. 23-35 (in Russian).
- Page, R.A., Boore, D.M. and Dieterich, J.H., 1975. Estimation of bedrock motion at ground surface. Geof. Surv. Prof. Paper 941A, Washington, US Govt. Print Off., 31-38.
- Rautian, T.G., 1976. A role of source function and medium response in the model of formation of seismic vibrations. In: Voprosy Inzhenernoi Seismologii, No.18, Moscow, Nauka, p.3-14 (in Russian).
- Shebalin, N.V., 1971. Comments on predominant period, spectrum and source of strong earthquake. In: Voprosy Inzhenernoi Seismologii, No.15, Moscow, Nauka, p. 50-78.
- Seismicheskoye Mikroraiionirovanie, 1977, Moscow, Nauka, p.34 (in Russian).
- Trifunac, M.D., 1976. Preliminary empirical model for scaling Fourier amplitude spectra of strong ground motion in terms of earthquake magnitude, source to station distance and recording site conditions. Bull. Seismol. Soc. Amer., v. 66, p. 1343-1373.
- Zapolskii, K.K., Zhbrykunova, N.A., Zhbrykunov, V.Ya. and Loginova, G.M., 1973. Spectral content of P waves of strong earthquakes. In: Zemletryaseniya v SSSR v 1969g. Moscow, Nauka, p. 220-227 (in Russian).
- Zapolskii, K.K., Nersesov, I.L., Rautian, T.G. and Khal-turin, V.I., 1974. The physical basis for magnitude classification of earthquakes. In: Magnituda i Energeticheskaya Klassifikatsiya Zemletryaseniya, I, Moscow, Nauka, p. 79-132 (in Russian).

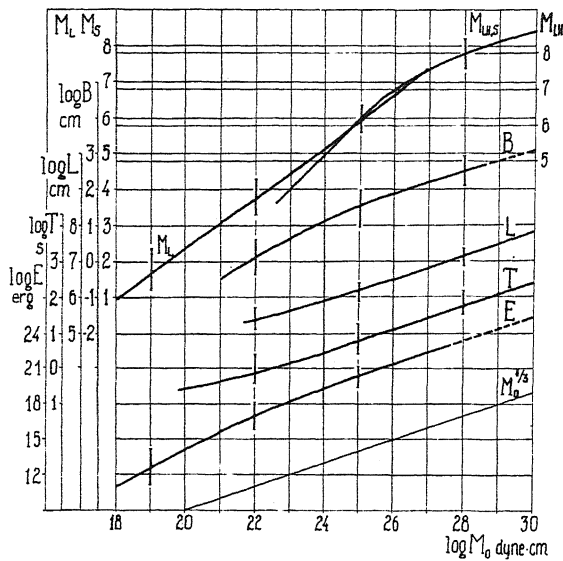


Fig. 1. Average relations between magnitudes M_L , M_S , M_{LH} , $M_{LH,S}$, average slip B , source length L , characteristic time T (reciprocal of corner frequency, or duration) and total energy compiled from different sources. Bars denote approximate range of real data.

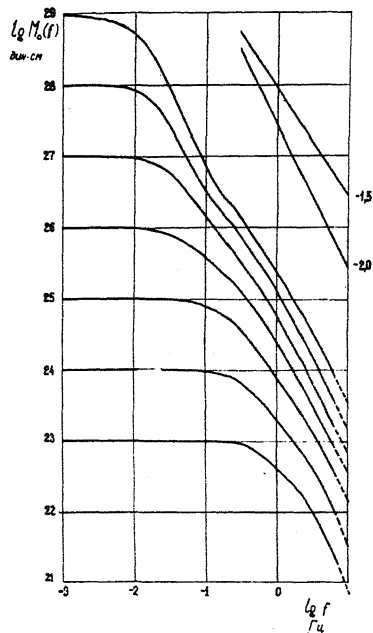


Fig. 2. Average source radiation spectra in terms of seismic moment spectrum of equivalent point source $M_0(f)$. $M_0 = M(0)$. Range of real spectra on the slope is about half order of magnitude.

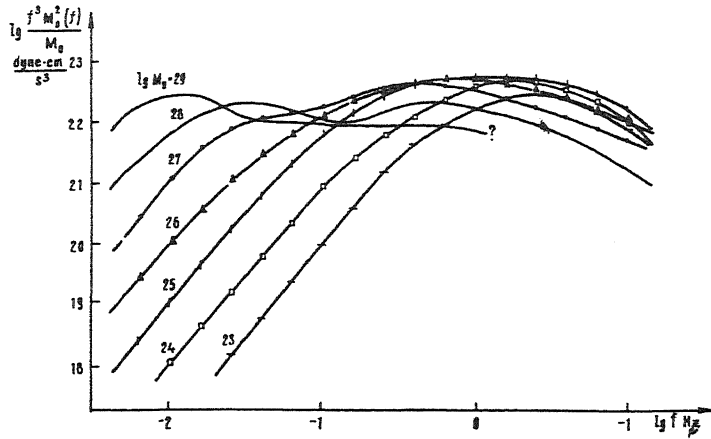


Fig. 3. Values of $f^3 M_0^2(f)/M_0$, which are proportional to radiant flux spectrum $W(f) = \frac{\partial^3 E}{\partial S \partial t \partial \log f}$ for set of M_0 values.

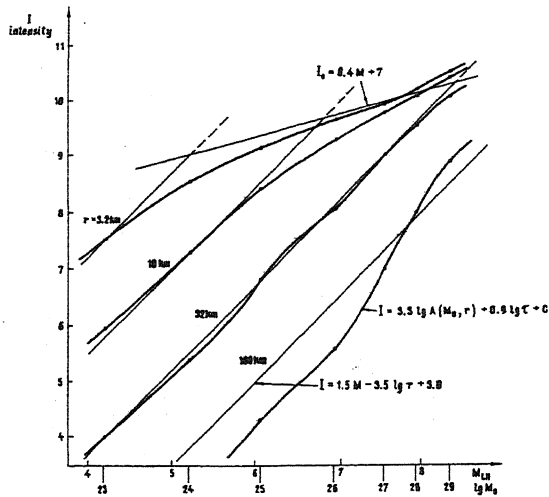


Fig. 4. Theoretical (curves) and smoothed empirical (straight lines) intensity I dependence upon magnitude M_{LH} for four values of distance. Theoretical I values included arbitrary constant and the best fit position of theoretical curves was chosen.

FLOW CHART FOR ACCELEROGRAM SIMULATION

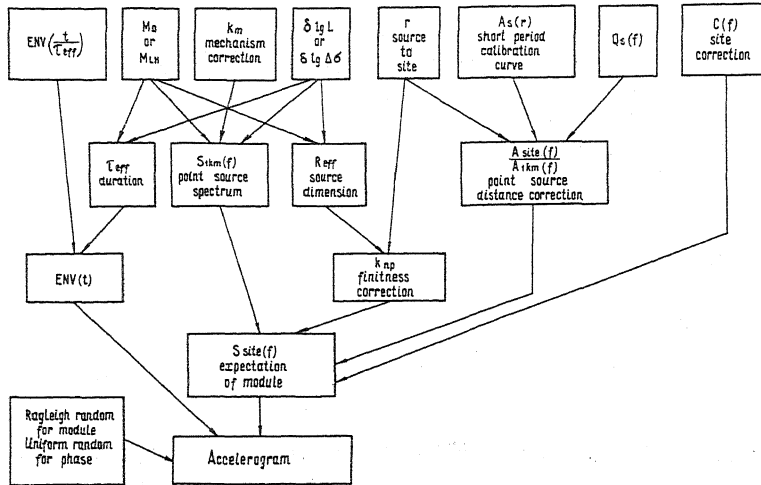


Fig. 5. Flow chart of simulation system.

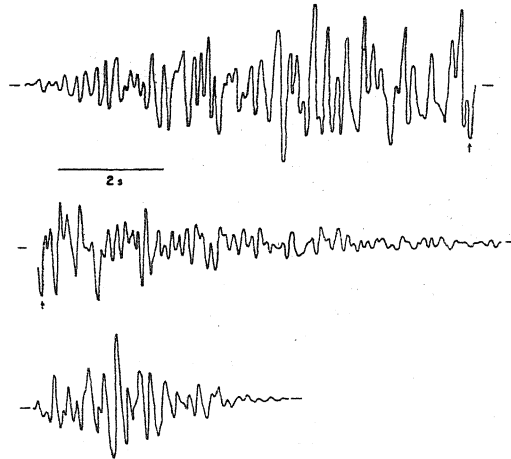


Fig. 6. Two examples of simulator output in the test run (filtered with passband $0.3 \pm 7\text{Hz}$).
 Upper traces: $M_0 = 25.6$, $r = 10 \text{ km}$, $A = 320 \text{ GAL}$;
 Lower trace: $M_0 = 23.7$, $r = 1 \text{ km}$, $A = 550 \text{ GAL}$.